NANJING UNIVERSITY

Exploring the Depths of Nuclear Matter with an Extended Linear Sigma Model

Presenter: Yao Ma (马垚)

In collaboration with Prof. Yong-Liang Ma (马永亮)

Hunan University, Changsha, Oct. 21st

Outline

- Motivation (Why extend the linear sigma model to dense system)
- Theoretical framework and phenomenological analysis (Nuclear matter properties and neutron star structures)
- Summary and outlook

誠樸雄偉 勵學敦行

Motivation

Rich phenomenons of dense environments

Weak parameterizations in past studies on nuclear matter

Nuclei structures (low/intermediate densities)

- Hadron interactions around saturation density $n_0 = 0.16\mathrm{fm}^{-3}$ are crucial to nuclei structures, e.g. $^{24}\mathrm{Mg}$, $^{90}\mathrm{Zr}$, $^{116}\mathrm{Sn}$ and ^{208} Pb

南京大學

B. A. Li and C. M. Ko, Nucl. Phys. A 618, 498 (1997).
D. H. Youngblood, H. L. Clark, and Y. W. Lui, Phys. Rev. Lett. 82, 691 (1999).
A. W. Steiner and B. A. Li, Phys. Rev. C 72, 041601 (2005).
L. W. Chen, C. M. Ko, and B. A. Li, Phys. Rev. C 72, 064309 (2005).
A. E. L. Dieperink, Y. Dewulf, D. Van Neck, M. Waroquier, and V. Rodin, Phys. Rev. C 68, 064307 (2003).
S. Karataglidis, K. Amos, B. A. Brown, and P. K. Deb, Phys. Rev. C 65, 044306 (2002).
R. J. Furnstahl, Nucl. Phys. A 706, 85 (2002).
B. A. Brown, Phys. Rev. Lett. 85, 5296 (2000).

$$E(n,\alpha) = E_0(n) + E_{\mathrm{sym}}(n)\alpha^2 + O\left(\alpha^4\right)$$

$$\alpha = \left(n_n - n_p\right)/\left(n_n + n_p\right)$$

$$n = n_n + n_p$$

$$E_0(n) = \boxed{E_0\left(n_0\right)} + \frac{\boxed{K_0}}{2!}\chi^2 + \frac{\boxed{J_0}}{3!}\chi^3 + O\left(\chi^4\right)$$

A. Sedrakian, J. J. Li, and F. Weber, Prog. Part. Nucl. Phys. 131, 104041 (2023)
M. Dutra, *et.al,* Phys. Rev. C 85, 035201 (2012).
J. M. Lattimer and Y. Lim, Astrophys. J. 771, 51 (2013).
M. Farine, J. M. Pearson, and F. Tondeur, Nucl. Phys. A 615, 135 (1997).

$$E_{\mathrm{sym}}(n) = \boxed{E_{\mathrm{sym}}\left(n_r\right)} + \boxed{L\left(n_r\right)}\chi_r + O\left(\chi_r^2\right)$$

$$\chi \equiv \left(n - n_0\right)/3n_0$$

$$\mathscr{L}_I = \bar{\psi}\left[i\gamma_\mu\partial^\mu - M - g_\sigma\sigma - g_\omega\gamma_\mu\omega^\mu - g_\rho\gamma_\mu\tau_a\rho^{a\mu}\right]\psi$$

$$\begin{aligned}
n_0 &\to 0.155 \pm 0.050\left(\mathrm{fm}^{-3}\right)\\
E_0(n_0) &\to -15.0 \pm 1.0(\mathrm{MeV})\\
E_{\mathrm{sym}}(n_0) &\to 30.9 \pm 1.9(\mathrm{MeV})\\
K_0 &\to 230 \pm 30(\mathrm{MeV})\\
L_0 &\to 52.5 \pm 17.5(\mathrm{MeV})\\
J_0 &\to -700 \pm 500(\mathrm{MeV})
\end{aligned}$$

嚴謹求實
勤奮創新

Neutron star (high densities)

- The density in the cores of NSs always reach nearly $8n_0$
- M-R relations/ tidal deformations are sensitive to the EOS behavior throughout the whole density regions

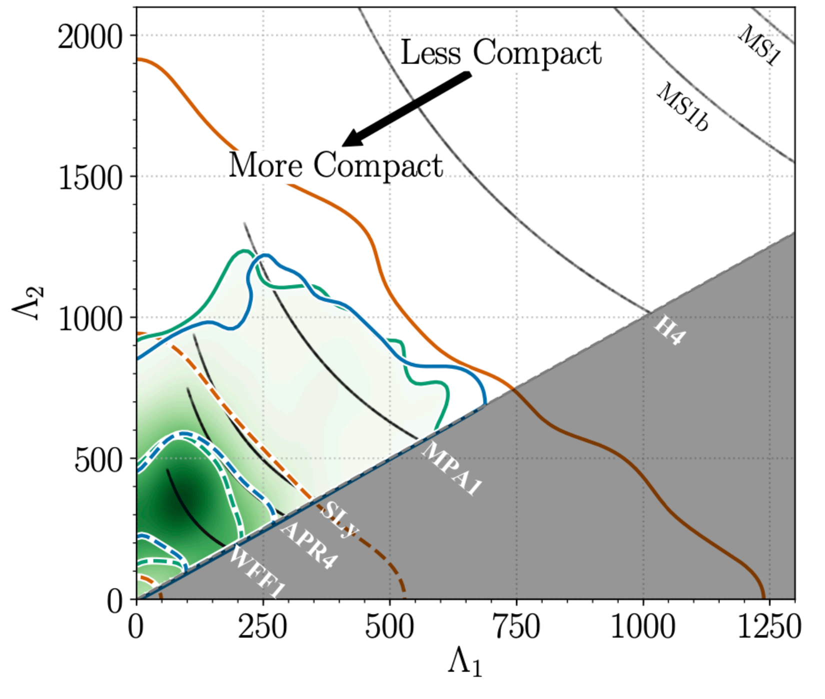

FIG. 1. Marginalized posterior for the tidal deformabilities of the two binary components of GW170817. The green shading shows the posterior obtained using the $\Lambda_a(\Lambda_s, q)$ EOS-insensitive relation to impose a common EOS for the two bodies, while the green, blue, and orange lines denote 50% (dashed) and 90% (solid) credible levels for the posteriors obtained using EOS-insensitive relations, a parametrized EOS without a maximum mass requirement, and independent EOSs (taken from [52]), respectively. The gray shading corresponds to the unphysical region $\Lambda_2 < \Lambda_1$ while the seven black scatter regions give the tidal parameters predicted by characteristic EOS models for this event [113, 115, 121–125].

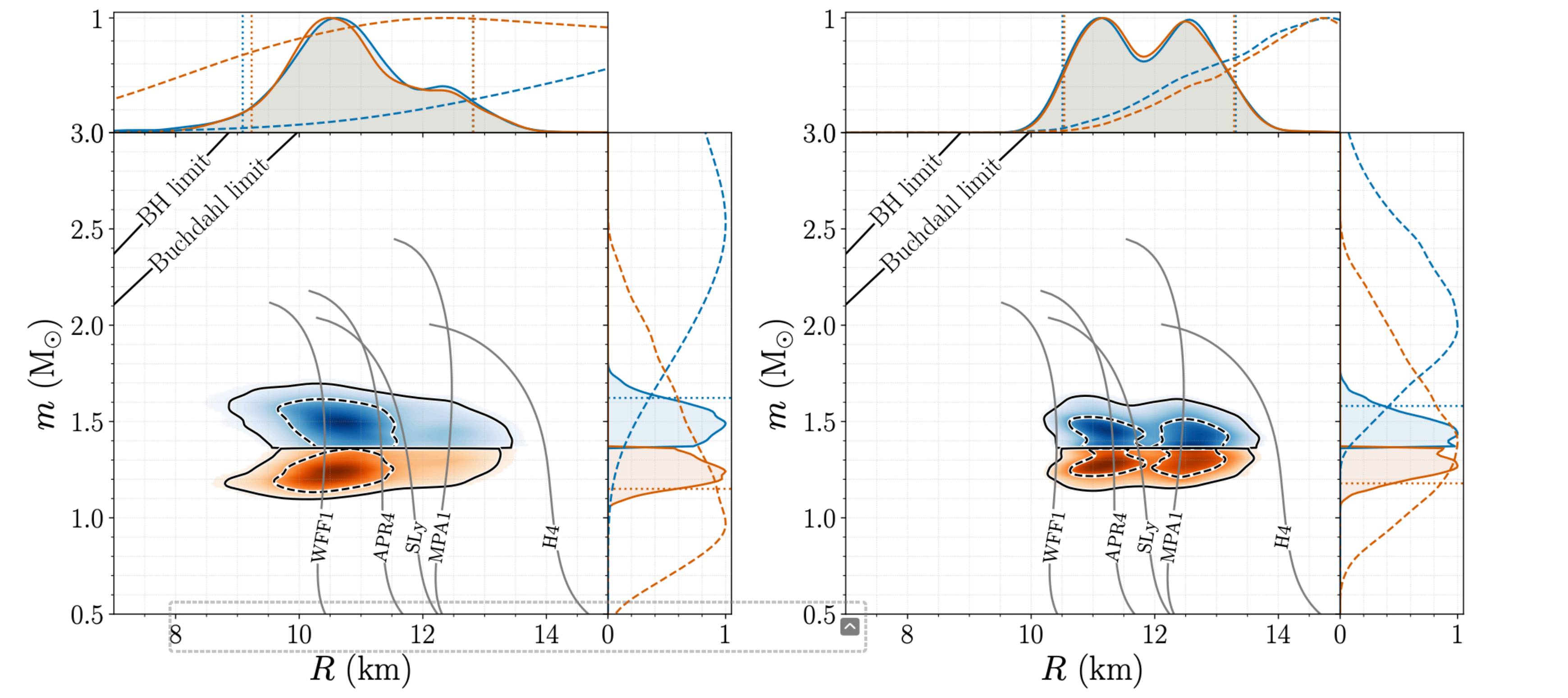

FIG. 3. Marginalized posterior for the mass m and areal radius R of each binary component using EOS-insensitive relations (left panel) and a parametrized EOS where we impose a lower limit on the maximum mass of 1.97 $M_\odot$ (right panel). The top blue (bottom orange) posterior corresponds to the heavier (lighter) NS. Example mass-radius curves for selected EOSs are overplotted in gray. The lines in the top left denote the Schwarzschild BH ($R = 2m$) and Buchdahl ($R = 9m/4$) limits. In the one-dimensional plots, solid lines are used for the posteriors, while dashed lines are used for the corresponding parameter priors. Dotted vertical lines are used for the bounds of the 90% credible intervals.

TABLE I. Source properties for GW170817: we give ranges encompassing the 90% credible intervals for different assumptions of the waveform model to bound systematic uncertainty. The mass values are quoted in the frame of the source, accounting for uncertainty in the source redshift.

	Low-spin priors ($\lvert\chi\rvert \leq 0.05$)	High-spin priors ($\lvert\chi\rvert \leq 0.89$)
Primary mass m_1	1.36–1.60 $M_\odot$	1.36–2.26 $M_\odot$
Secondary mass m_2	1.17–1.36 $M_\odot$	0.86–1.36 $M_\odot$
Chirp mass $\mathcal{M}$	$1.188^{+0.004}_{-0.002} M_\odot$	$1.188^{+0.004}_{-0.002} M_\odot$
Mass ratio m_2/m_1	0.7–1.0	0.4–1.0
Total mass $m_{\rm tot}$	$2.74^{+0.04}_{-0.01} M_\odot$	$2.82^{+0.47}_{-0.09} M_\odot$
Radiated energy $E_{\rm rad}$	$> 0.025 M_\odot c^2$	$> 0.025 M_\odot c^2$
Luminosity distance $D_{\rm L}$	40^{+8}_{-14} Mpc	40^{+8}_{-14} Mpc
Viewing angle Θ	$\leq 55°$	$\leq 56°$
Using NGC 4993 location	$\leq 28°$	$\leq 28°$
Combined dimensionless tidal deformability $\tilde{\Lambda}$	≤ 800	≤ 700
Dimensionless tidal deformability $\Lambda(1.4 M_\odot)$	≤ 800	≤ 1400

B. P. Abbott et al. (LIGO Scientific, Virgo), Phys. Rev. Lett. 119, 161101 (2017)
B. P. Abbott et al. (LIGO Scientific, Virgo), Phys. Rev. Lett. 121, 161101 (2018)

Polytropic process + strong interaction constructions

QCD at low energy regions

嚴謹求實
勤奮創新

- Rich phenomenons at hadron sectors which can't be described directly by solving QCD because of non-perturbative property

- Methods to solve QCD at low energies:

A. OBE-type models (leading order estimation)

B. Lattice QCD (high temperature, low density, the first principle)

C. Chiral EFT (high temperature, high density, approximation)

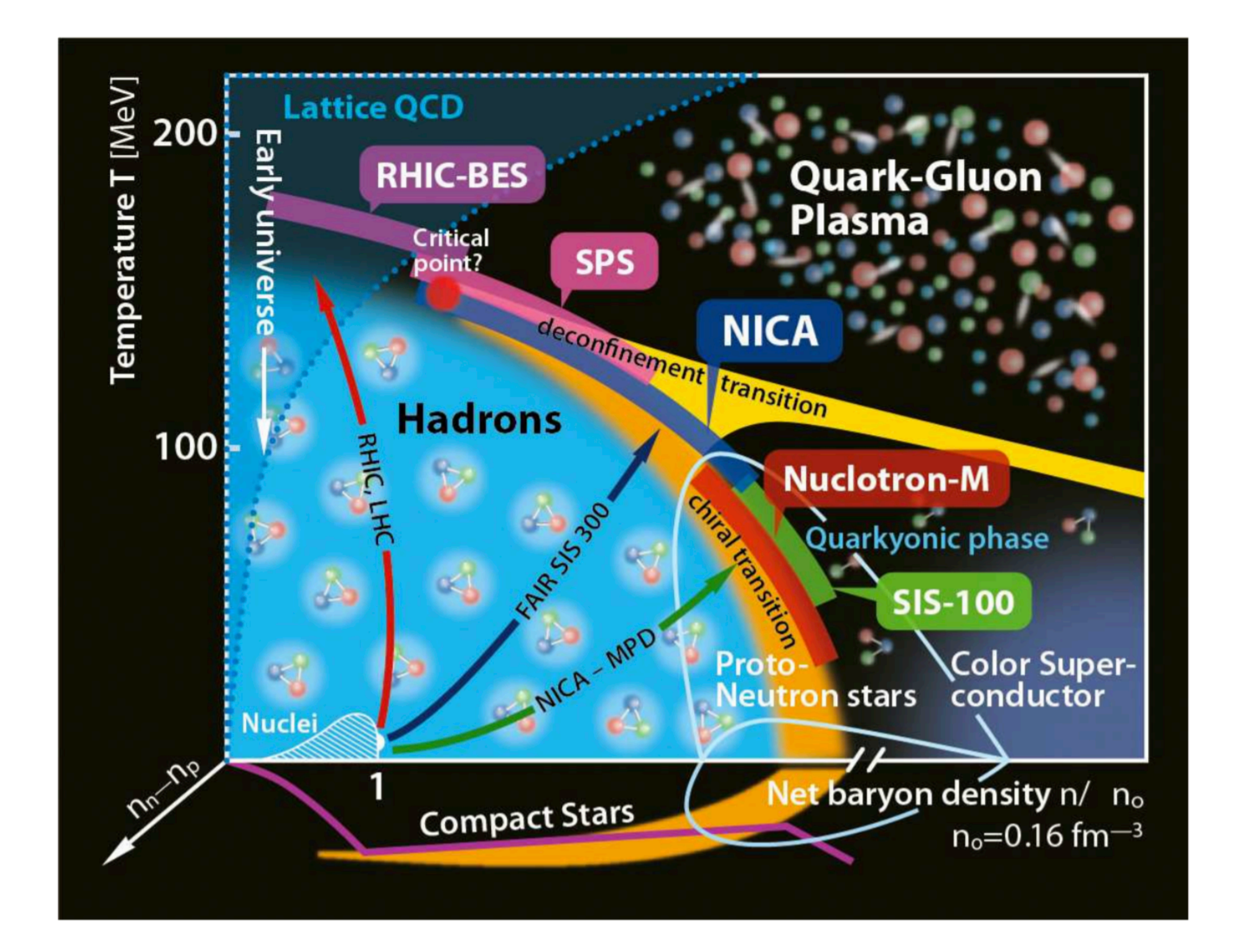

L. Turko, Universe 4, 52 (2018)

Method to handle dense system

1. Relativistic mean field approximation

J. D. Walecka, Ann. Phys. **83**, 491 (1974).

$$
\begin{aligned}
\mathscr{L} &= \mathscr{L}_{\mathrm{N}} + \mathscr{L}_{\sigma} + \mathscr{L}_{\omega} + \mathscr{L}_{\mathrm{I}} \\
\mathscr{L}_{\mathrm{N}} &= \bar{\psi}\left(\mathrm{i}\gamma_\mu\partial^\mu - m_{\mathrm{N}}\right)\psi \\
\mathscr{L}_{\sigma} &= \frac{1}{2}\left(\partial_\mu\phi\partial^\mu\phi - m_\sigma^2\phi^2\right) \\
\mathscr{L}_{\omega} &= -\frac{1}{4}W_{\mu\nu}W^{\mu\nu} + \frac{1}{2}m_\omega^2\omega_\mu\omega^\mu \\
\mathscr{L}_{\mathrm{I}} &= \mathscr{L}_{\sigma\mathrm{N}} + \mathscr{L}_{\omega\mathrm{N}} = g_\sigma\phi\bar{\psi}\psi - g_\omega\omega^\mu\bar{\psi}\gamma_\mu\psi
\end{aligned}
$$

$$
\begin{aligned}
&\left(\mathrm{i}\gamma_\mu\partial^\mu - g_\omega\gamma_0\omega^0 - m_{\mathrm{N}}\right)\psi = 0, \quad m_{\mathrm{N}}^* = m_{\mathrm{N}} - g_\sigma\phi, \\
&\phi = \frac{g_\sigma}{m_\sigma^2}\rho_{\mathrm{s}}, \quad \rho_{\mathrm{s}} = \langle\bar{\psi}\psi\rangle, \\
&\omega^0 = \frac{g_\omega}{m_\omega^2}\rho_{\mathrm{B}}, \quad \rho_{\mathrm{B}} = \left\langle\psi^\dagger\psi\right\rangle,
\end{aligned}
$$

2. Hatree-Fock method

$$
\begin{aligned}
\mathscr{L}_I = &-g_\sigma\bar{\psi}\sigma\psi - g_\omega\bar{\psi}\gamma_\mu\omega^\mu\psi + \frac{f_\omega}{2M}\bar{\psi}\sigma_{\mu\nu}\partial^\nu\omega^\mu\psi \\
&-g_\rho\bar{\psi}\gamma_\mu\rho^\mu\cdot\tau\psi + \frac{f_\rho}{2M}\bar{\psi}\sigma_{\mu\nu}\partial^\nu\rho^\mu\cdot\tau\psi \\
&-e\bar{\psi}\gamma_\mu\frac{1}{2}\left(1+\tau_3\right)A^\mu\psi + \mathscr{L}_{\pi\mathrm{NN}}
\end{aligned}
$$

$$\Sigma(\mathbf{p}) = \Sigma_S(p) + \gamma_0\Sigma_0(p) + \gamma\cdot\hat{\mathbf{p}}\Sigma_V(p)$$

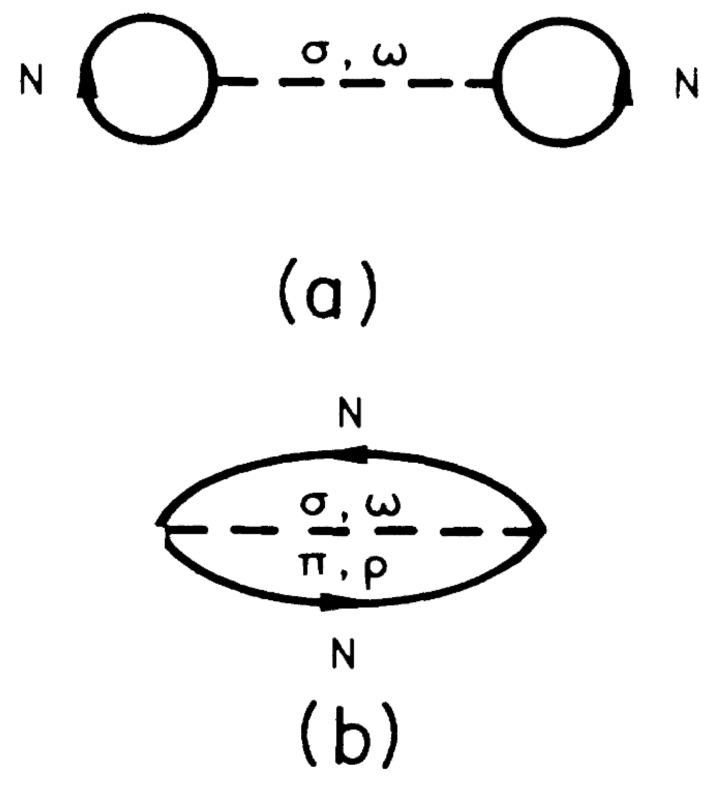

A. Bouyssy, J.-F. Mathiot, N. V. Giai, and S. Marcos, Phys Rev C **36**, 380 (1987).

誠樸雄偉 勵學敦行

Can we extend an EFT/model taking care of QCD symmetry patterns into dense nucleon systems?

An extended linear sigma model in nuclear matter

Phys. Rev. D 109 (2024) 7, 7, **YM** and Y. L. Ma

P-wave problems in light scalar meson sectors below 1GeV

F. E. Close and N. A. Tornqvist, J. Phys. G 28, R249 (2002)

↓

A tetra-quark picture to include δ ($a_0(980)$) meson and hyperon

Freedoms to be considered

- Highlights of the parametrization:

I. Include meson exchanges, e.g. $f_0(500)(\sigma)$ and $a_0(980)(\delta)$

II. Include baryon freedoms, e.g. nucleon and hyperon

$$R^\mu = V^\mu - A^\mu = \frac{1}{\sqrt{2}}\begin{pmatrix} \frac{\omega_N^\mu+\rho^{\mu 0}}{\sqrt{2}} - \frac{f_{1N}^\mu + a_1^{\mu 0}}{\sqrt{2}} & \rho^{\mu +} - a_1^{\mu +} & K^{*\mu +} - K_1^{\mu +} \\ \rho^{\mu -} - a_1^{\mu -} & \frac{\omega_N^\mu-\rho^{\mu 0}}{\sqrt{2}} - \frac{f_{1N}^\mu - a_1^{\mu 0}}{\sqrt{2}} & K^{*\mu 0} - K_1^{\mu 0} \\ K^{*\mu -} - K_1^{\mu -} & \bar{K}^{*\mu 0} - \bar{K}_1^{\mu 0} & \omega_S^\mu - f_{1S}^\mu \end{pmatrix}$$

$$L^\mu = V^\mu + A^\mu = \frac{1}{\sqrt{2}}\begin{pmatrix} \frac{\omega_N^\mu+\rho^{\mu 0}}{\sqrt{2}} + \frac{f_{1N}^\mu + a_1^{\mu 0}}{\sqrt{2}} & \rho^{\mu +} + a_1^{\mu +} & K^{*\mu +} + K_1^{\mu +} \\ \rho^{\mu -} + a_1^{\mu -} & \frac{\omega_N^\mu-\rho^{\mu 0}}{\sqrt{2}} + \frac{f_{1N}^\mu - a_1^{\mu 0}}{\sqrt{2}} & K^{*\mu 0} + K_1^{\mu 0} \\ K^{*\mu -} + K_1^{\mu -} & \bar{K}^{*\mu 0} + \bar{K}_1^{\mu 0} & \omega_S^\mu + f_{1S}^\mu \end{pmatrix}$$

$$\Phi = S + iP = \begin{pmatrix} \frac{(\sigma_N + a_0^0) + i(\eta_N + \pi^0)}{\sqrt{2}} & a_0^+ + i\pi^+ & K_S^+ + iK^+ \\ a_0^- + i\pi^- & \frac{(\sigma_N - a_0^0) + i(\eta_N - \pi^0)}{\sqrt{2}} & K_S^0 + iK^0 \\ K_S^- + iK^- & \bar{K}_S^0 + i\bar{K}^0 & \sigma_S + i\eta_S \end{pmatrix}$$

a_0 mesons may be crucial to NS tidal deformations and neutron skin of nucleus

D. Adhikari et al. (PREX), Phys. Rev. Lett. 126, 172502 (2021)
B. T. Reed, F. J. Fattoyev, C. J. Horowitz, and J. Piekarewicz, Phys. Rev. Lett. 126, 172503 (2021)
F. Li, B. J. Cai, Y. Zhou, W. Z. Jiang, and L. W. Chen, Astrophys. J. 929, 183 (2022)

$$B_N \equiv \begin{pmatrix} \frac{\Lambda}{\sqrt{6}} + \frac{\Sigma^0}{\sqrt{2}} & \Sigma^+ & p \\ \Sigma^- & \frac{\Lambda}{\sqrt{6}} - \frac{\Sigma^0}{\sqrt{2}} & n \\ \Xi^- & \Xi^0 & -\frac{2\Lambda}{\sqrt{6}} \end{pmatrix}$$

High densities may lead to hyperon cores of NSs

N. K. Glendenning, Astrophys. J. 293, 470 (1985)
N. K. Glendenning and S. A. Moszkowski, Phys. Rev. Lett. 67, 2414 (1991).
S. Weissenborn, D. Chatterjee, and J. Schaffner-Bielich, Phys. Rev. C 85, 065802 (2012), [Erratum: Phys. Rev. C 90, 019904 (2014)]

The Lagrangian at the lowest order for RMF

A. H. Fariborz, R. Jora, and J. Schechter, Phys. Rev. D 72, 034001 (2005)
A. H. Fariborz, R. Jora, and J. Schechter, Phys. Rev. D 77, 034006 (2008)
A. H. Fariborz, R. Jora, and J. Schechter, Phys. Rev. D 79, 074014 (2009)

$$\mathrm{U(1)_A}$$

$$\underbrace{\boxed{\Phi}}_{\text{2-quark}} \to \boxed{e^{2i\nu}}\Phi, \quad \underbrace{\boxed{\hat{\Phi}}}_{\text{4-quark}} \to \boxed{e^{-4i\nu}}\hat{\Phi}$$

$$\begin{aligned}\mathscr{L}_{\mathrm{V}} = {} & h_2 \,\mathrm{Tr}\left(V^2 S^2\right) + g_3 \,\mathrm{Tr}\, V^4 \\ & + a_1 \epsilon_{abc}\epsilon_{def} V_{ad} V_{be}\left(S^2\right)_{cf} \\ & + a_2 \epsilon_{abc}\epsilon_{def} V_{ad} V_{be}\left(V^2\right)_{cf}\end{aligned}$$

$$\mathscr{L}_{\mathrm{M}} = -c_2 \mathrm{Tr} S^2 + d_2 \mathrm{Tr} \hat{S}^2 + c_4 \mathrm{Tr} S^4 + 2 e_3 \epsilon_{abc}\epsilon_{def} S_{ad} S_{be} \hat{S}_{cf}$$

Di-quark approximations

$$\begin{aligned}\mathscr{L}_{\mathrm{B}} = {} & \mathrm{Tr}\left(\bar{B} i \gamma_\mu \partial^\mu B\right) + c \,\mathrm{Tr}\left(\bar{B}\gamma^0 V B\right) - g \,\mathrm{Tr}\left(\bar{B} S B\right) \\ & + h \epsilon_{abc}\epsilon_{def} \bar{B}_{ad}\gamma^0 B_{be} V_{cf} \\ & - e \epsilon_{abc}\epsilon_{def} \bar{B}_{ad}\gamma^0 B_{be} S_{cf}\end{aligned}$$

Phys. Rev. D 109 (2024) 7, 7, **YM** and Y. L. Ma

Improvement of parameter space

SSB of chiral symmetry

◉ Spontaneous symmetry breaking down from $\mathrm{SU(3)_L} \otimes \mathrm{SU(3)_R}$ to $\mathrm{SU(3)_V}$

$$\boxed{\left\langle S_a^b \right\rangle = \alpha_a \delta_a^b, \quad \left\langle \hat{S}_a^b \right\rangle = \beta_a \delta_a^b}$$

◉ Mixing between 2-quark and 4-quark configurations

$$\boxed{\begin{bmatrix} \phi_{i,j} \\ \hat{\phi}_{i,j} \end{bmatrix} = R \begin{bmatrix} \phi'_{i,j} \\ \hat{\phi}'_{i,j} \end{bmatrix} = \begin{bmatrix} \cos\theta_{i,j} & -\sin\theta_{i,j} \\ \sin\theta_{i,j} & \cos\theta_{i,j} \end{bmatrix} \begin{bmatrix} \phi'_{i,j} \\ \hat{\phi}'_{i,j} \end{bmatrix}}$$

Phenomenological analysis

Parameter space choice

	α(MeV)	β(MeV)	e_3(MeV)	c_4	h_2	g_3	c	g	a_1	h	e
g3-0eg	61.4	26.4	-2100	45.6	79.3	0.397	9.51	6.54	4.10	-2.61	8.75
g3-0e	61.1	24.4	-2050	43.6	80.0	0.542	11.4	0.234	4.17	-0.790	15.1
g3-0g	61.1	24.7	-2060	44.0	80.1	1.59	-0.792	15.4	4.25	11.5	-0.027
g3-50eg	61.2	25.6	-2100	44.4	79.9	51.5	10.1	6.35	4.14	-2.65	9
g3-100eg	60.8	24.0	-2090	42.4	80.8	100	10.6	7.10	4.19	-2.88	8.34
g3-150eg	60.7	24.3	-2110	42.0	81.0	150	11.1	7.15	4.18	-3.05	8.30

$g_{\sigma NN}$	g_{aNN}	g_{fNN}	$g_{\omega NN}$	$g_{\rho NN}$
-5.98	-0.671	2.68	6.06	3.45
-6.20	-5.03	3.00	6.09	5.30
-6.17	5.12	2.95	-6.09	5.30
-6.12	-0.852	2.85	6.37	3.71
-6.36	-0.442	3.19	6.73	3.85
-6.38	-0.413	3.20	7.09	4.04

Bare mass parameters and NM properties

嚴謹求實
勤奮創新

Y. Sugahara and H. Toki, Nucl. Phys. A579,557 (1994).
F. Li, B. J. Cai, Y. Zhou, W. Z. Jiang, and L. W. Chen, Astrophys. J. 929, 183 (2022).

Physical quantities in unit of MeV

	B.E.	$E_{\rm sym}$	K_0	L_0	J_0	m_ρ	m_ω	m_σ	$m_{\sigma'}$	m_{a_0}	$m_{a_0'}$	m_N
Empirical	-15.0±1.0	30.9±1.9	250±50	52.5±17.5	-700±500	763±2	783±1	475±75	1350±100	995±25	1410±120	939±1
g3-0eg	-14.6	30.1	415	92.2	421	763	783	503	1520	977	1510	939
g3-0e	-14.6	31.6	420	85.8	479	763	783	525	1510	991	1480	939
g3-0g	-14.6	30.9	418	83.6	451	763	783	522	1510	989	1480	939
g3-50eg	-15.2	30.9	370	80.7	-392	763	783	498	1520	983	1500	939
g3-100eg	-15.4	31.4	317	71.7	-1020	763	783	502	1510	994	1470	939
g3-150eg	-15.6	31.6	253	63.7	-1470	763	783	485	1510	991	1470	939
TM1	-16.3	36.9	280	113	-247	770	783	511	—	—	—	938
$\mathrm{FSU}-\delta 6.7$	-16.3	32.7	229	53.5	-322	763	783	492	—	980	—	938

A. Sedrakian, J. J. Li, and F. Weber, Prog. Part. Nucl. Phys. 131, 104041 (2023).
J. M. Lattimer and Y. Lim, Astrophys. J. 771, 51 (2013).
M. Farine, J. M. Pearson, and F. Tondeur, Nucl. Phys. A 615, 135 (1997).
M. Dutra, et al., Phys. Rev. C 85, 035201 (2012).

R. L. Workman, et al. (Particle Data Group), PTEP 2022, 083C01 (2022).

Comparison with Walecka-type models

嚴謹求實
勤奮創新

Saturation density

A. Sedrakian, J. J. Li, and F. Weber, Prog. Part. Nucl. Phys. 131, 104041 (2023)

	Empirical	ELSM	TM1	$\mathrm{FSU}-\delta 6.7$
$n_0(\mathrm{fm}^{-}3)$	0.155±0.005	0.155	0.145	0.148

Symmetric nuclear matter

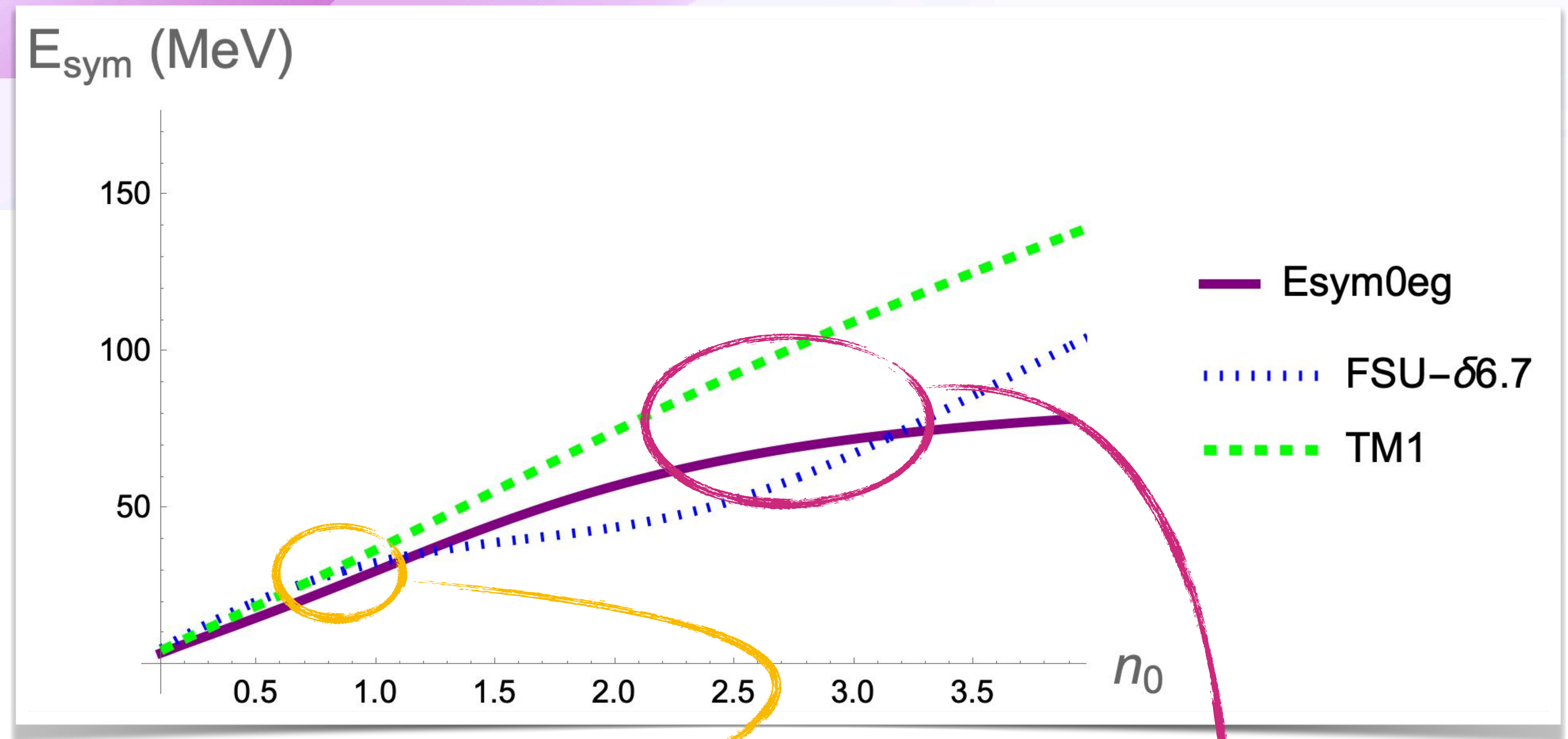

Pure neutron matter

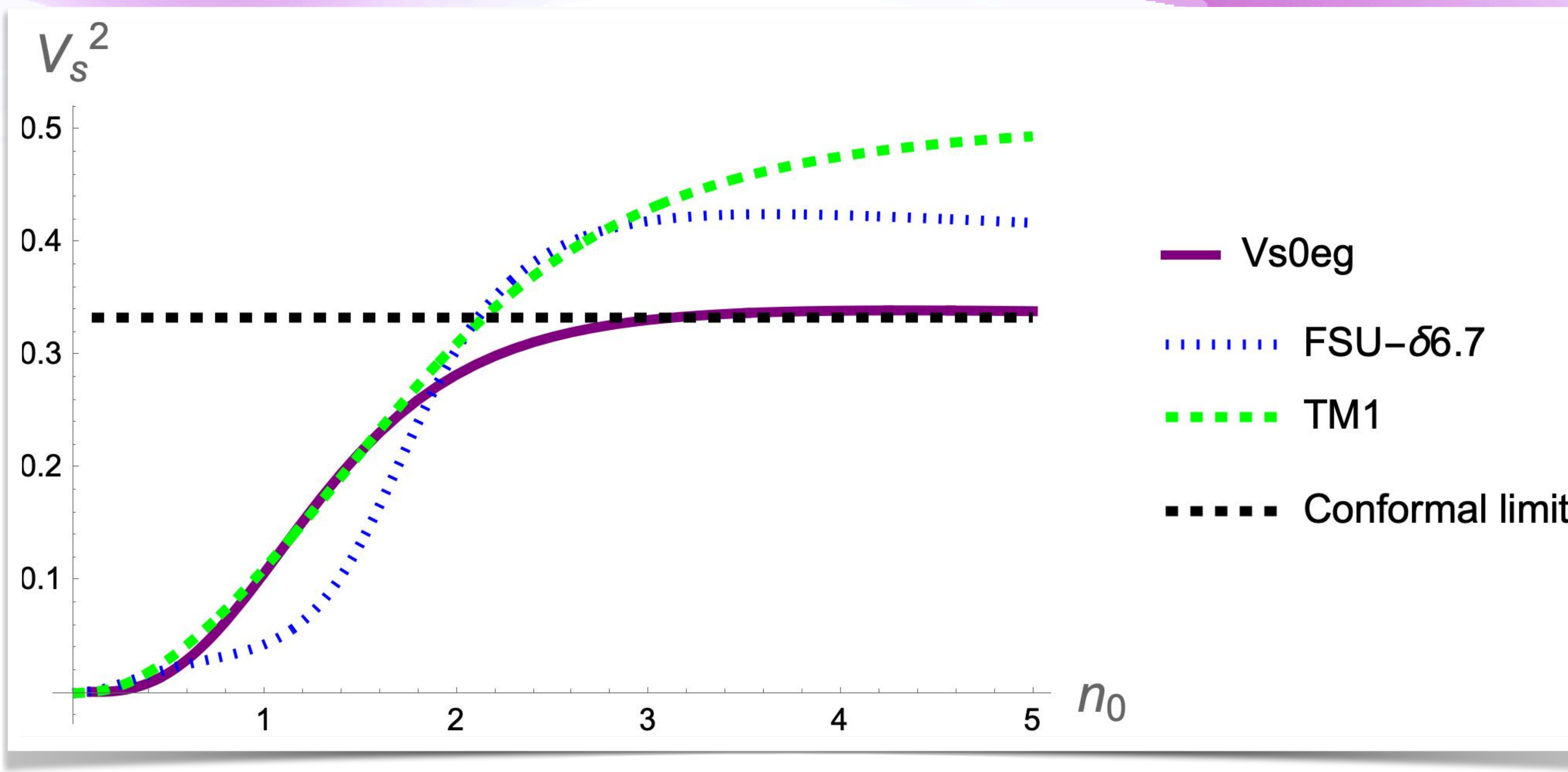

$L\left(2/3n_0\right) \geq 49\mathrm{MeV}$

GW170817 $\Lambda_{1.4} \leq 580$

D. Adhikari et al., PREX, Phys. Rev. Lett. 126, 172502 (2021)
B. T. Reed, F. J. Fattoyev, C. J. Horowitz, and J. Piekarewicz, Phys. Rev. Lett. 126, 172503 (2021)

B. P. Abbott et al., LIGO Scientific, Virgo, Phys. Rev. Lett. 121, 161101 (2018)

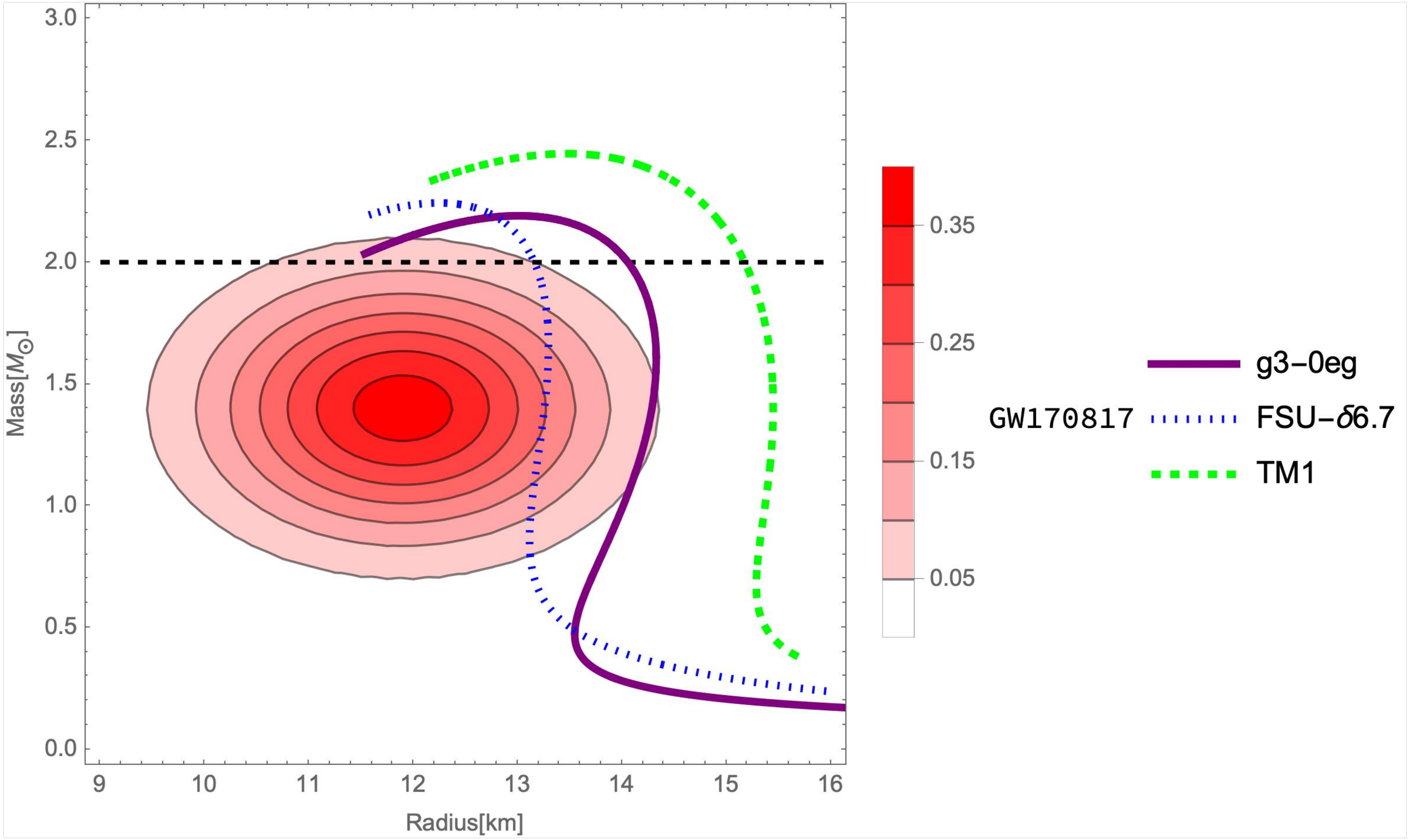

3.0
2.5
2.0
1.5
1.0
0.5
0.0
Mass[$M_\odot$]
9
10
11
12
13
14
15
16
Radius[km]
0.35
0.25
0.15
0.05
GW170817
g3−0eg
FSU−δ6.7
TM1

Comparison among different g_{aNN} cases

嚴謹求實
勤奮創新

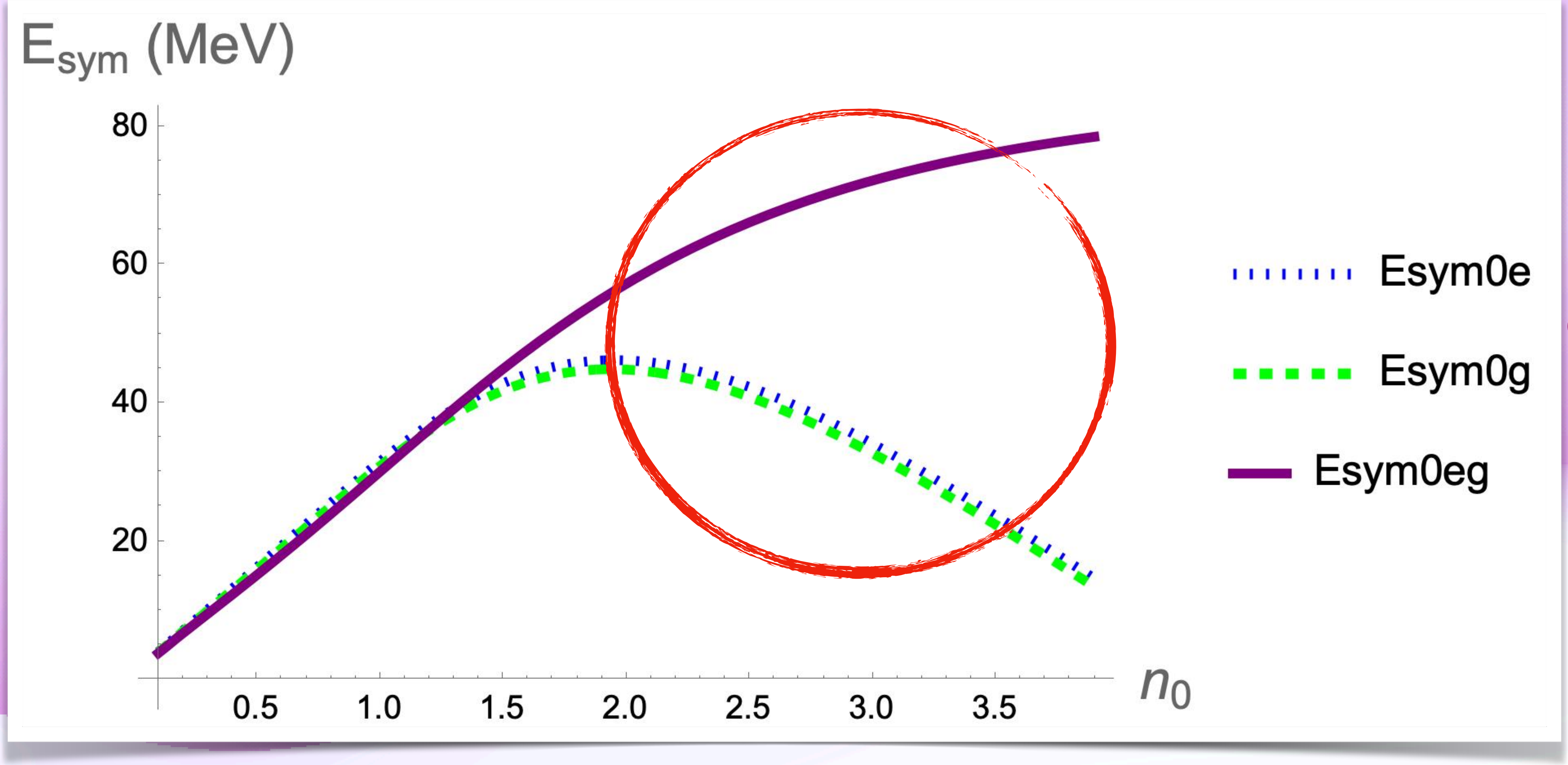

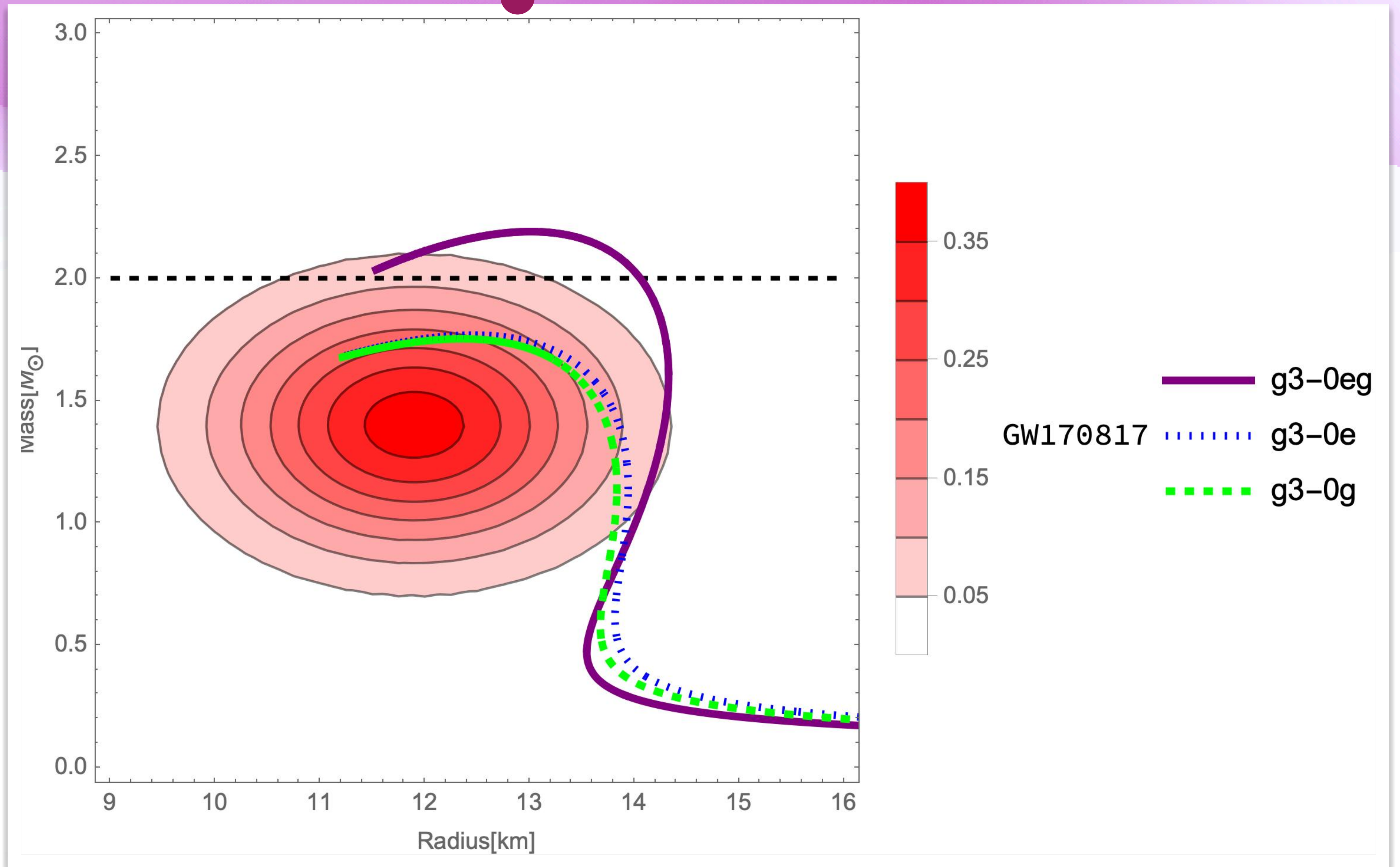

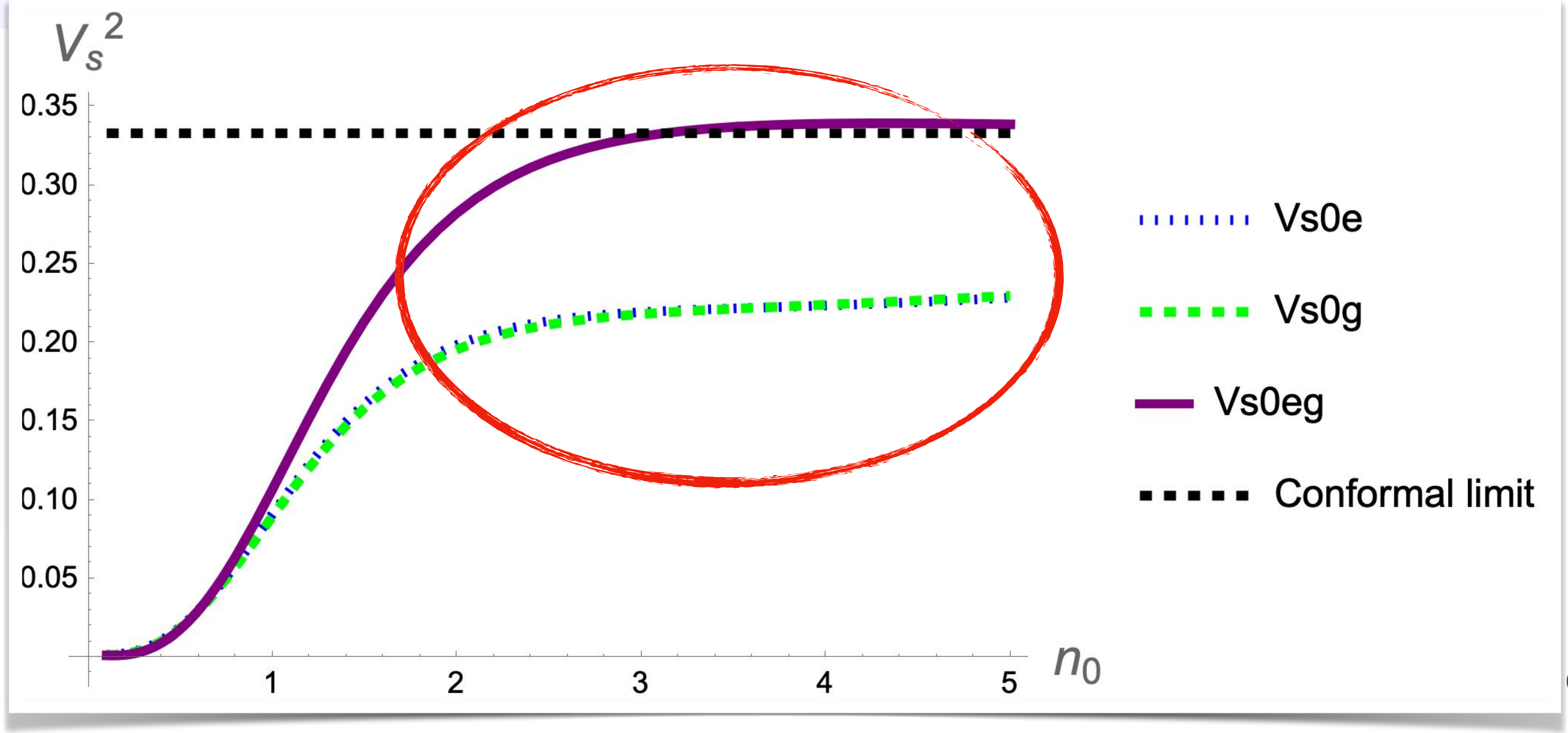

Comparison among different g_3 cases

嚴謹求實
勤奮創新

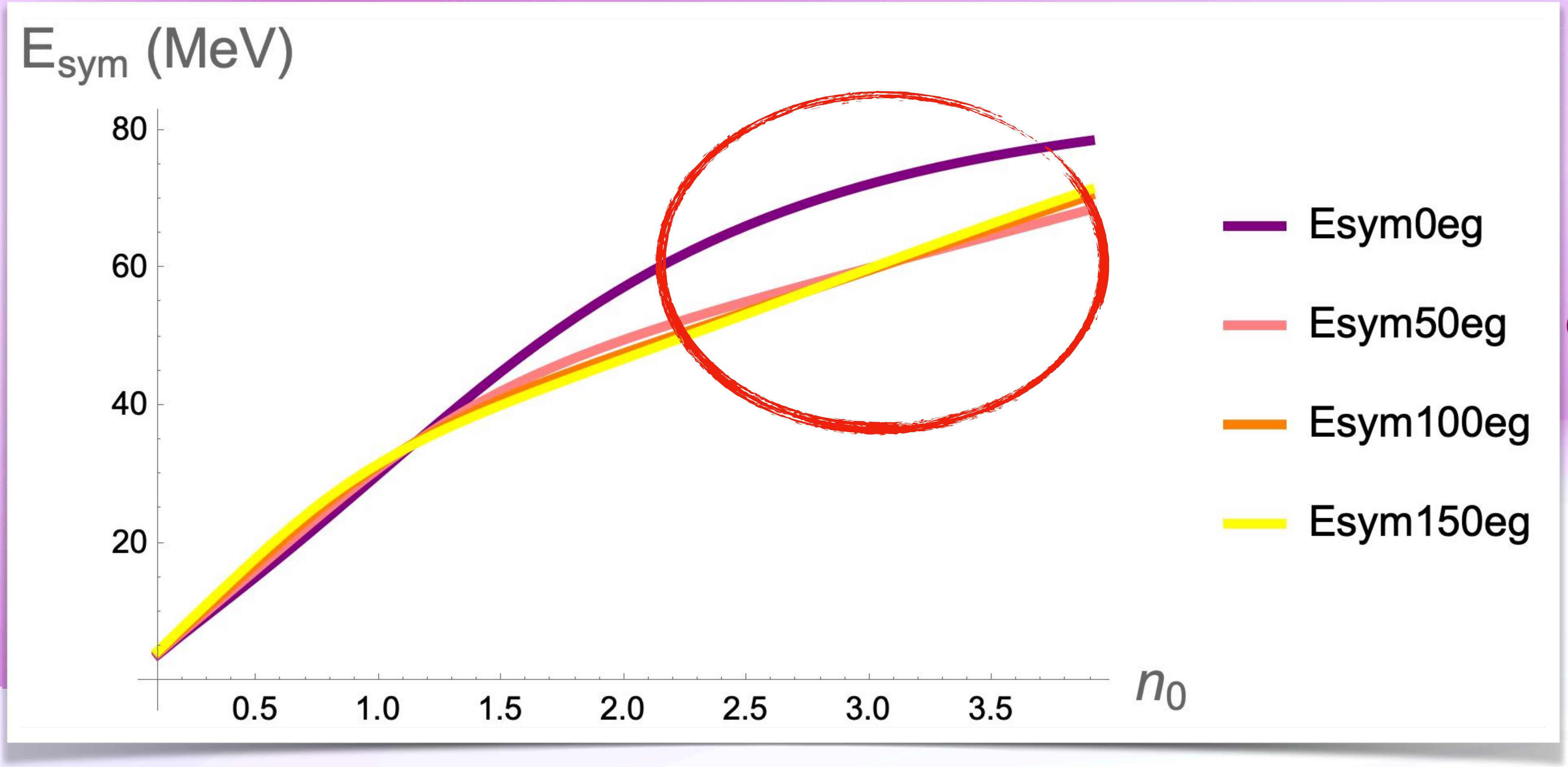

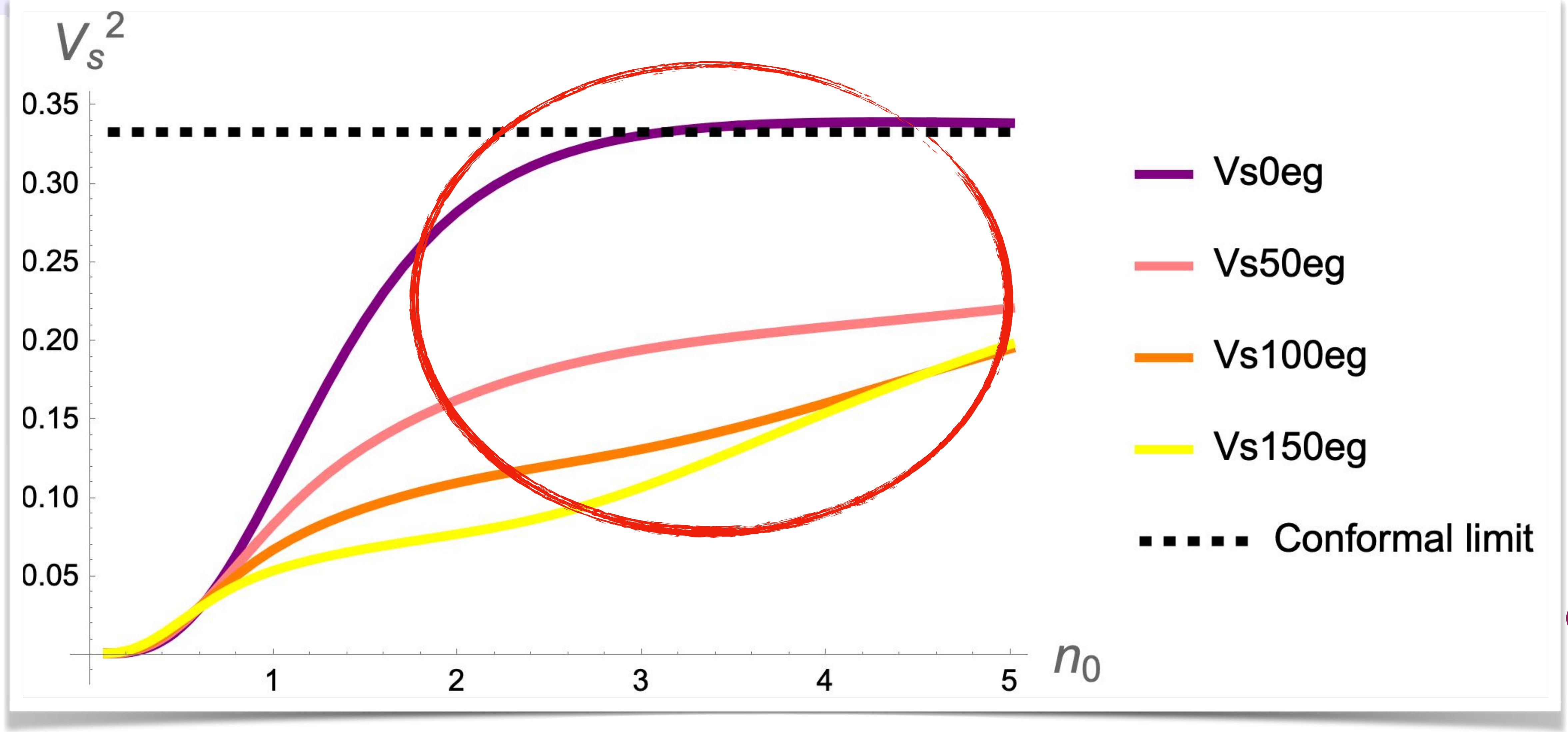

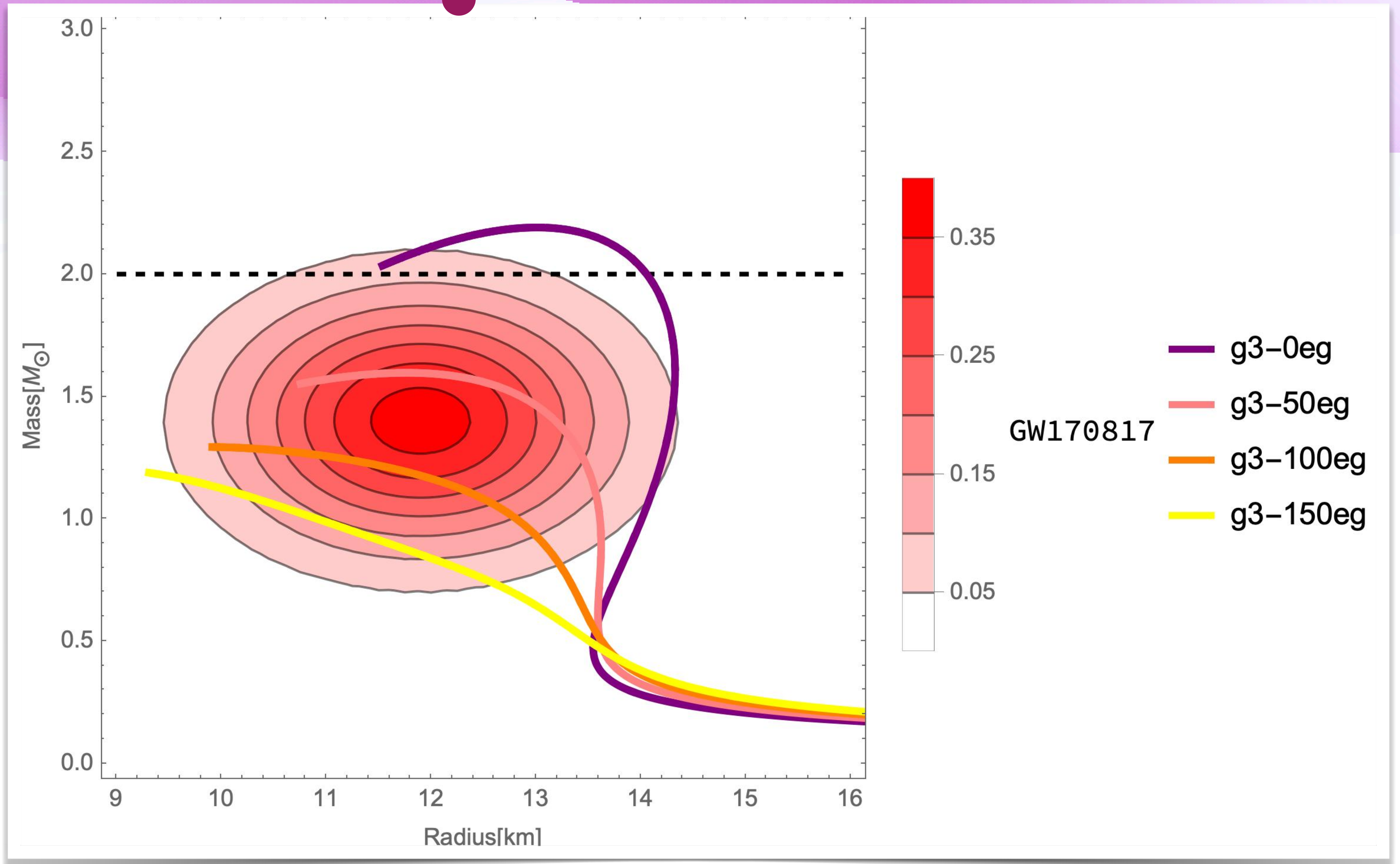

Summary and outlook

I. The extended linear sigma model can reproduce nuclear matter (NM) properties around saturation density while accounting for chiral symmetry patterns;

II. Regarding the well-reproduced vacuum spectra and NM properties at low densities, different parameter space choices significantly affect the neutron star (NS) structure;

III. These astrophysical objects may serve as a promising test field for strong interaction theories/models, with more detailed analysis forthcoming.

Thank you!

Backup

Chiral Representation

- (pseudo-)scalar mesons:

$$\Phi = S + iP = \begin{pmatrix} \frac{(\sigma_N + a_0^0) + i(\eta_N + \pi^0)}{\sqrt{2}} & a_0^+ + i\pi^+ & K_S^+ + iK^+ \\ a_0^- + i\pi^- & \frac{(\sigma_N - a_0^0) + i(\eta_N - \pi^0)}{\sqrt{2}} & K_S^0 + iK^0 \\ K_S^- + iK^- & \bar{K}_S^0 + i\bar{K}^0 & \sigma_S + i\eta_S \end{pmatrix}$$

2-quark state 4-quark state

$$\boxed{\Phi} \to g_L \Phi g_R^\dagger, \quad \boxed{\hat{\Phi}} \to g_L \hat{\Phi} g_R^\dagger$$

- (axial-)vector mesons:

$$R^\mu = V^\mu - A^\mu = \frac{1}{\sqrt{2}} \begin{pmatrix} \frac{\omega_N^\mu + \rho^{\mu 0}}{\sqrt{2}} - \frac{f_{1N}^\mu + a_1^{\mu 0}}{\sqrt{2}} & \rho^{\mu +} - a_1^{\mu +} & K^{*\mu +} - K_1^{\mu +} \\ \rho^{\mu -} - a_1^{\mu -} & \frac{\omega_N^\mu - \rho^{\mu 0}}{\sqrt{2}} - \frac{f_{1N}^\mu - a_1^{\mu 0}}{\sqrt{2}} & K^{*\mu 0} - K_1^{\mu 0} \\ K^{*\mu -} - K_1^{\mu -} & \bar{K}^{*\mu 0} - \bar{K}_1^{\mu 0} & \omega_S^\mu - f_{1S}^\mu \end{pmatrix}$$

$$L^\mu = V^\mu + A^\mu = \frac{1}{\sqrt{2}} \begin{pmatrix} \frac{\omega_N^\mu + \rho^{\mu 0}}{\sqrt{2}} + \frac{f_{1N}^\mu + a_1^{\mu 0}}{\sqrt{2}} & \rho^{\mu +} + a_1^{\mu +} & K^{*\mu +} + K_1^{\mu +} \\ \rho^{\mu -} + a_1^{\mu -} & \frac{\omega_N^\mu - \rho^{\mu 0}}{\sqrt{2}} + \frac{f_{1N}^\mu - a_1^{\mu 0}}{\sqrt{2}} & K^{*\mu 0} + K_1^{\mu 0} \\ K^{*\mu -} + K_1^{\mu -} & \bar{K}^{*\mu 0} + \bar{K}_1^{\mu 0} & \omega_S^\mu + f_{1S}^\mu \end{pmatrix}$$

$$L_\mu \to g_L L_\mu g_L^\dagger, \quad R_\mu \to g_R R_\mu g_R^\dagger$$

Baryons:

$$B_N \equiv \begin{pmatrix} \frac{\Lambda}{\sqrt{6}} + \frac{\Sigma^0}{\sqrt{2}} & \Sigma^+ & p \\ \Sigma^- & \frac{\Lambda}{\sqrt{6}} - \frac{\Sigma^0}{\sqrt{2}} & n \\ \Xi^- & \Xi^0 & -\frac{2\Lambda}{\sqrt{6}} \end{pmatrix}$$

$$N_R^{(RR)} \to g_R N_R^{(RR)} g_R^\dagger, \quad N_L^{(RR)} \to g_L \boxed{N_L^{(RR)}} g_R^\dagger$$

$$N_R^{(LL)} \to g_R N_R^{(LL)} g_L^\dagger, \quad N_L^{(LL)} \to g_L N_L^{(LL)} g_L^\dagger$$

$$N_R^{(RR)} \to e^{-3iv} N_R^{(RR)}, \quad N_L^{(RR)} \to e^{-iv} N_L^{(RR)},$$

$$N_R^{(LL)} \to e^{iv} N_R^{(LL)}, \quad N_L^{(LL)} \to e^{3iv} N_L^{(LL)}$$

Diquark approximation

$$B = \frac{1}{\sqrt{2}} \left(N^{(RR)} - N^{(LL)} \right)$$

$$= \frac{1}{\sqrt{2}} \left(N_L^{(RR)} + N_R^{(RR)} - N_R^{(LL)} - N_L^{(LL)} \right)$$

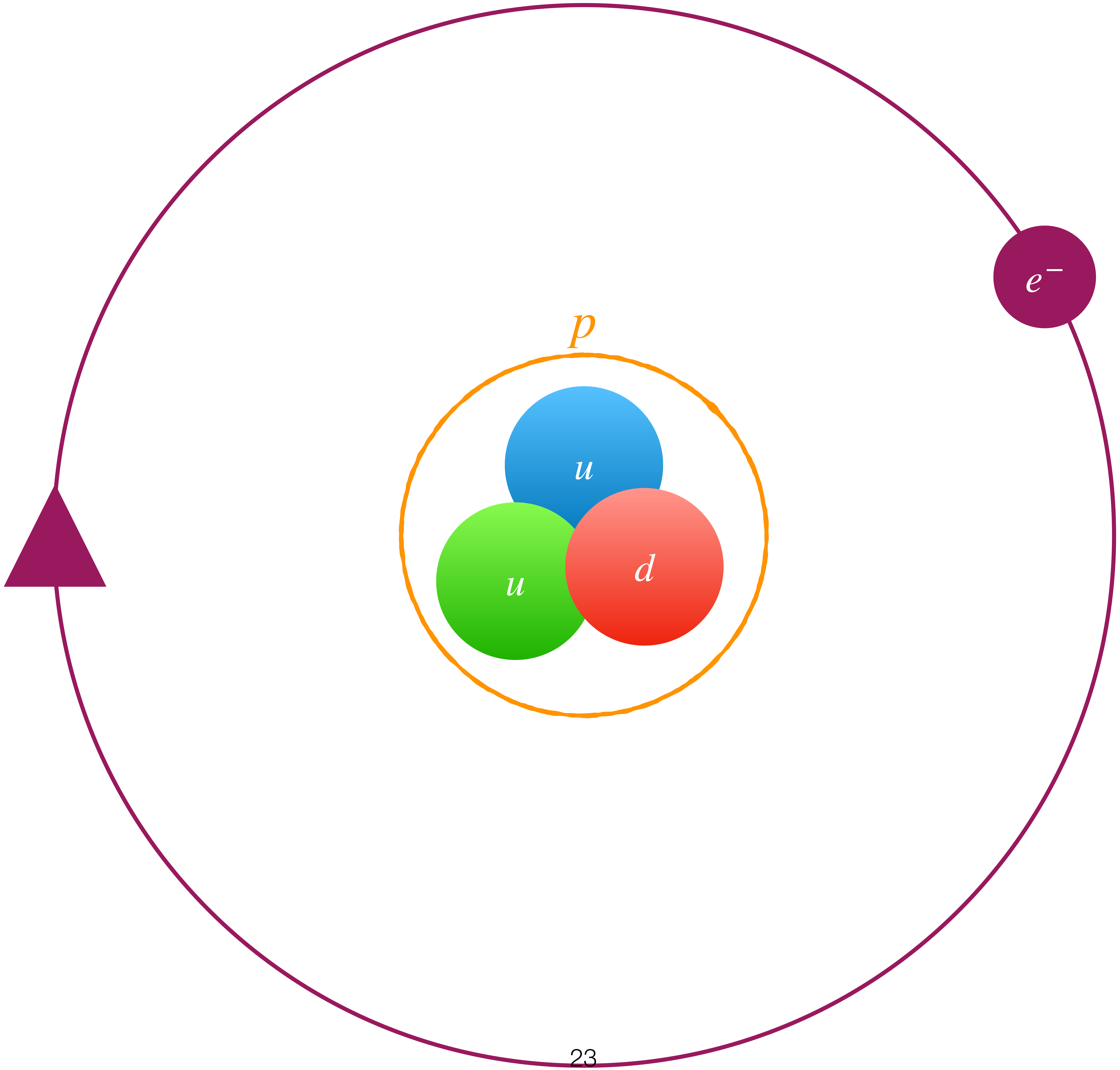
e^-
p
u
u
d